

Analytical Methods

Accepted Manuscript



This is an *Accepted Manuscript*, which has been through the Royal Society of Chemistry peer review process and has been accepted for publication.

Accepted Manuscripts are published online shortly after acceptance, before technical editing, formatting and proof reading. Using this free service, authors can make their results available to the community, in citable form, before we publish the edited article. We will replace this *Accepted Manuscript* with the edited and formatted *Advance Article* as soon as it is available.

You can find more information about *Accepted Manuscripts* in the [Information for Authors](#).

Please note that technical editing may introduce minor changes to the text and/or graphics, which may alter content. The journal's standard [Terms & Conditions](#) and the [Ethical guidelines](#) still apply. In no event shall the Royal Society of Chemistry be held responsible for any errors or omissions in this *Accepted Manuscript* or any consequences arising from the use of any information it contains.



Analytical Methods

PAPER

Detection of epinephrine and metanephrine at nitrogen doped three-dimensional porous graphene modified electrode

Received 00th January 20xx,
Accepted 00th January 20xx

DOI: 10.1039/x0xx00000x

www.rsc.org/

Qi Yang, Yang Zhao, Jie Bai, Liping Wu, Hui-Min Zhang,* and Liangti Qu*

Abstract: A nitrogen doped three-dimensional porous graphene (NG) modified electrode was fabricated in our work. The electrochemical characterization by the voltammetric behavior of hexaamineruthenium chloride ($\text{Ru}(\text{NH}_3)_6\text{Cl}_3$) showed that the redox peak currents were significantly enhanced at the modified electrode compared with that of bare GCE, which was ascribed to the excellent properties of NG. Meanwhile, distinguishing electrocatalysis was observed for epinephrine (EP) and metanephrine (MEP) at the modified electrode. The redox mechanisms of EP and MEP were researched and proposed. The modified electrode can be used for sensitive detection of EP and MEP. By differential pulse voltammetry, the anodic peak currents were linearly proportional to the concentrations from 1.0 μM to 1.0 mM with a sensitivity of 0.021 $\mu\text{A}/\mu\text{M}$ for EP and 1.5 μM to 0.41 mM with a sensitivity of 0.0095 $\mu\text{A}/\mu\text{M}$ for MEP. The detection limits were ascertained to be 0.67 μM and 1.3 μM for EP and MEP, respectively. Additionally, the detection of EP and MEP was possible in the presence of ascorbic acid and uric acid. The modified electrode showed good stability, reproducibility and repeatability, and was applied to the detection of EP and MEP in human plasma samples with recoveries from 98.9% to 100.9%, and EP hydrochloride injections with recoveries from 100.3% to 104.6%.

1. Introduction

Epinephrine (EP), an important catecholamine neurotransmitter in the mammalian central nervous system, plays an vital role during the time of stress.^{1,2} The concentration of EP in human bodies is closely relative to many diseases, like parkinsonism. Additionally, EP is always used as an usual emergency health-care medicine to relieve the symptom of faint heartbeat, hypotension, dyspnoea, and so on. Metanephrine (MEP) is a metabolite of EP during the interaction with a kind of transferase. The measurement of MEP is considered to be the first line biochemical diagnosis of pheochromocytomas and paragangliomas,^{3,4} which will give rise to hypertension directly. So, the detection of EP and MEP seems extremely important in clinical medicine. The current test methods include radioimmunoassay,⁵ high performance liquid chromatography,⁶ fluorescence⁷ and capillary electrophoresis.⁸ Due to high sensitivity, reproducibility, simpler procedures and ease of miniaturization,⁹ electrochemical biosensors were explored to determine EP.^{10,11} But no electrochemical sensor was found for the detection of MEP.

Graphene is one-atom-thick planar sheet of sp^2 -hybridized conjugated carbon atoms which are compactly packed in a honeycomb crystal lattice.^{12,13} It has been widely developed to electrode modification due to its excellent electrochemical properties in recent years.¹⁴⁻¹⁶ Nevertheless, the graphene sheets on the electrode usually assemble layer-by-layer owing to their strong π - π interaction, yielding a compact film.¹⁷ Such compact film would not only reduce the specific surface area, but hinder the rapid diffusion of electrolyte. Also, in some previous works,^{18,19} graphene exhibits slow electron transfer rate due to its low edge plane content, which will result in blocking underlying electron transfer of the modified electrodes. In order to solve the above problems, three-dimensional (3D) graphene has attracted significant attentions due to its large surface area and tunable configuration.^{20,21} In addition, its beneficial structure with oriented edges, achievable for efficient adsorption and faster electron transfer rate has drawn wide attention to the application of electrochemical biosensors which exhibit high electrocatalytic activity.²² However, the absence of band gap of graphene results in uncontrollability on its conductivity which will limit its application in electrochemistry. Nitrogen doping into the carbon lattice of graphene has been considered to be an efficient way to improve the electrochemical properties of graphene.²³⁻²⁵ With nitrogen doping into graphene successfully, the band gap of graphene between the valence band and the conduction band will be opened, endowing

*School of Chemistry, Beijing Institute of Technology, Beijing 100081, China. E-mail: huimin@bit.edu.cn, lqu@bit.edu.cn; Tel: +86-10-68912668

† Electronic supplementary information (ESI) available. See DOI: 10.1039/x0xx00000x

nitrogen doped graphene with good conductivity.²⁶ The edge structure and chemical terminations became more controllable when they were made into semiconductors.²⁷ In addition, nitrogen doped graphene acted better photocatalytic efficiency for its narrow band gap and more active region.²⁸ Recently, it has been used as an effective material for electrochemical biosensors and showed remarkably improved electrocatalytic capability.^{29,30}

As is well known, EP undergoes electrochemical redox processes at graphene, graphene oxide or graphene nanosheet modified electrodes,^{12,31,32} and good behavior was obtained. But seldom results were used as the sensor to detect EP. Additionally, there is no result for MEP. Here, we introduced nitrogen doped 3D porous graphene modified electrode to response EP and MEP. The results will be proved to offer a low overpotential oxidation and remarkably current enhancement effect for EP and MEP and the sensor results were given.

2. Experimental

2.1. Reagents

EP and MEP were purchased from Sigma-Aldrich and were dissolved in double distilled water when used. As supporting electrolyte, 0.1 M PBS with different pH values were prepared by mixing the solutions of 0.1 M K_2HPO_4 and 0.1 M NaH_2PO_4 . Chitosan (CS) was purchased from Sinopharm Chemical Reagent Co., Ltd (China) and the CS solution (0.5 wt.% in 2 wt.% acetic acid aqueous solution) was prepared in advance. All other chemicals not mentioned were analytical reagent grade.

2.2. Apparatus

Electrochemical experiments were performed with a CHI660D Electrochemical Workstation which was purchased from Shanghai Chenhua Instrument Corporation (China). A conventional three-electrode system was applied in our experiment throughout. A platinum electrode was performed as counter electrode, a saturated calomel electrode (SCE) served as reference electrode, a bare or modified glassy carbon electrode (GCE) (3 mm in diameter) was employed as working electrode. All of the solutions will be removed oxygen before electrochemical measurements. The modified films were characterized by FEI Quanta 250FEG scanning electron microscopy (SEM) (America). Raman spectra were recorded with a Jobin Yvon HR-800 spectrometer from 500 to 4000 cm^{-1} .

2.3. Preparation of modified electrode

The synthetic method and detailed characterizations of NG used in our experiment were reported in our previous work.³³ The NG was dissolved in ethanol to create 1.0 $mg mL^{-1}$ alcoholic solution when used. GCE was polished with 0.3 μm Al_2O_3 powder. After rinsing with double distilled water, the polished electrode was sonicated with ethanol and double distilled water for 1 minute in turn, and then dried in air. The NG-chitosan-modified electrode (NG/CS/GCE) was made by casting 10 μL NG suspension (5 μL 0.5 wt.% CS solution and 5 μL 1.0 $mg mL^{-1}$ NG alcoholic solution) on the surface of GCE, then dried under an infrared lamp. Here, the mass of NG to

prepare the modified electrode was optimized as 5 μg (seen as Fig. S1).

2.4. Live subject statement

The authors state that all experiments were performed in compliance with the relevant laws and institutional guidelines. Institutional committee of Beijing Institute of Technology approved the experiments. The authors also state that informed consent was obtained for any experimentation with human subjects and Beijing Institute of Technology is committed to the protection and safety of human subjects involved in research.

3. Results and discussion

3.1. Characterization of NG/CS/GCE

We first view the morphological characterization of NG/CS/GCE via SEM. As illustrated in Fig. 1(A), NG was homogeneously coated on the surface of the electrode. The magnified SEM image (Fig. 1(B)) shows that the inherent 3D porous structure of NG still remains integrity. The diameters of pores are several micrometers, and the walls consist of thin layers of crumpled graphene sheets. This 3D porous structure possesses large specific surface area and interconnected network, which facilitates the diffusion of the electrolyte.³⁴

Raman spectroscopy (with 514 nm excitation) was carried out in order to have further insight into the above observations. The Raman spectrum of NG exhibits two characteristic peaks at around 1360 cm^{-1} and 1580 cm^{-1} which correspond to the well-defined D band and G band, respectively (Fig. 2). As we all know, the D band is related to the structural defects or graphene edges, while the G band is associated with the first-order scattering of the E_{2g} mode of sp^2 carbon domains. The intensity ratio of the D and G band (here

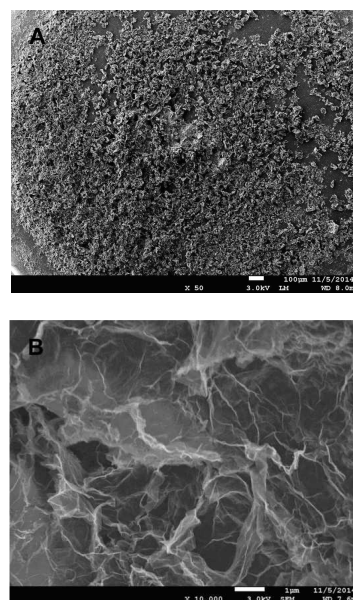


Fig. 1 (A) SEM image of the surface of NG/CS/GCE. (B) High-resolution SEM image of the surface of NG/CS/GCE.

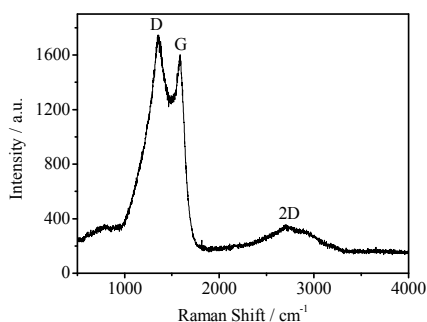


Fig. 2 Raman spectrum of NG

$I_D/I_G = 1.08$) indicates a large percentage of structural defects which may be a result of the nitrogen doped in the graphene. Furthermore, the intensity ratio of the G and 2D band (appears at around 2710 cm^{-1}) (here $I_G/I_{2D} = 4.59$) reveals that the NG is comprised of few layers graphene domains³⁵, which is consistent with SEM image of NG in Fig. 1(B).

Hexaammineruthenium chloride ($\text{Ru}(\text{NH}_3)_6\text{Cl}_3$) was chosen throughout the electrochemical characterization as an outer-sphere electron transfer redox probe, the redox of which is only dependent upon the electronic structure of carbon materials (graphene)^{36,37}. As shown in Fig. 3(A), there was a pair of redox waves at NG/CS/GCE and bare GCE, respectively. Although the apparent formal potentials of $\text{Ru}(\text{NH}_3)_6\text{Cl}_3$ at both the NG/CS/GCE and bare GCE (165 and 160 mV, respectively) were almost the same, the ΔE_p of NG/CS/GCE (50 mV) was much smaller than that of bare GCE (80 mV). Additionally, compared with bare GCE, the redox peak currents of NG/CS/GCE increased remarkably. These results reveal that NG/CS/GCE shows better electrochemical response, which could be ascribed to the unique porous architecture with large accessible active surface area. Furthermore, the appearance of the fast electron transfer rate observed at the modified electrode likely related to the large global percentage of edge plane like-sites/defects residing on the NG, which may due to the three-dimensional porous structure and the nitrogen doped in the graphene³⁸. Fig. 3(B) depicts the cyclic voltammograms (CVs) of $\text{Ru}(\text{NH}_3)_6\text{Cl}_3$ at different scan rates at NG/CS/GCE. It was shown that the redox peak currents were enhanced with the increase of the scan rate. Meanwhile, the peak potentials scarcely changed. The redox peak currents had a linear relationship with the square root of scan rate in the range of $10\text{--}500\text{ mV s}^{-1}$ (as shown in the inset of Fig. 3(B)), suggesting that the electrode process of $\text{Ru}(\text{NH}_3)_6\text{Cl}_3$ at NG/CS/GCE is a diffusion-controlled process. Besides, as is prospective for the case of the semi-infinite diffusion model which is governed by the Randles-Ševčík equation³⁹, $\log_{10} i_{pa}$ versus $\log_{10} \nu$ revealed the gradients of 0.56, viz a purely diffusional process without the thin-layer effects^{38,40}.

3.2. Electrochemical behaviors of epinephrine and metanephrine at NG/CS/GCE

3.2.1. Cyclic voltammograms of epinephrine and metanephrine

Considering that redox peaks induced from nitrogen doped graphene may be unstable due to the C-N bonding which may

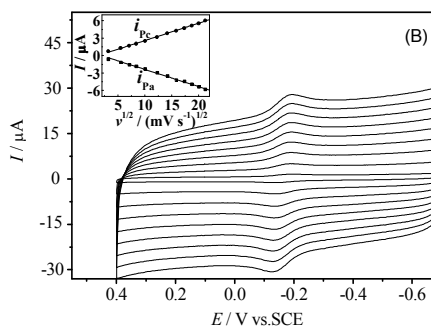
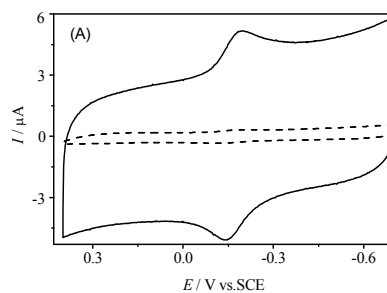


Fig. 3 (A) CVs of $1.0 \times 10^{-5}\text{ M Ru}(\text{NH}_3)_6\text{Cl}_3/0.1\text{ M KCl}$ solution at NG/CS/GCE (solid line) and bare GCE (dashed line) at 100 mV s^{-1} ; (B) CVs of $1.0 \times 10^{-5}\text{ M Ru}(\text{NH}_3)_6\text{Cl}_3/0.1\text{ M KCl}$ solution at NG/CS/GCE with different scan rates: 10, 50, 100, 150, 200, 250, 300, 400, 500 mV s^{-1} (from inner to outer). Inset: plots of the anodic and cathodic peak currents (i_{pa} and i_{pc}) vs. the square root of scan rate.

definitely affect the latter electrochemical reaction, baseline experiment was investigated in our work. Fig. S2 shows the CVs of blank PBS (0.1 M, pH 7.0) at NG/CS/GCE in the range of -1.0 V to 0.8 V . The baseline keeps almost unchanged after scanning 10 circles, which demonstrates that NG/CS/GCE fabricated in our work is stable in electrochemical scanning process.

Fig. 4 shows the CVs of EP at bare GCE and NG/CS/GCE in 0.1 M pH 7.0 PBS. It was seen that, a well-defined anodic peak (a1) and a cathodic peak (c2) can be observed in the first cycle, and another anodic peak (a2) was emerged in the continuous second cycle at both bare and modified GCE, which is consistent with the previous work.⁴¹ The anodic peak potential of a1 at bare GCE was 290 mV, while it was 180 mV at NG/CS/GCE. That is, the overpotential for the oxidation of EP at the modified electrode reduced 110 mV. ΔE_p , the difference between E_{pa2} and E_{pc2} , was 20 mV at NG/CS/GCE, which is much smaller than that of 83 mV at bare GCE. Besides, the redox peak currents of EP enhanced significantly at NG/CS/GCE, which may be attributed to the increase of the active surface area. While the reducing ΔE_p may due to the faster electron transfer rate causing from edge plane like-sites/defects and the nitrogen doped in the 3D graphene.

Some results previously obtained on other pure graphene-based modified electrodes for the electrochemical behavior study of EP were listed in Table 1. The 180 mV of anodic potential at NG/CS/GCE is much lower than that obtained

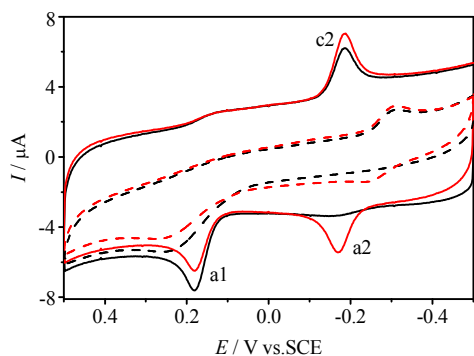


Fig. 4 CVs of 0.1 mM EP at bare GCE (dash line) and NG/CS/GCE (solid line) (the black and red lines corresponding to the first and continuous second cycle scans, respectively) in 0.1 M pH 7.0 PBS. Scan rate: 50 mV s^{-1} .

at most of other pure graphene-based modified electrodes. The low oxidation overpotential of EP may be ascribed to the significant electrocatalytic property of NG/CS/GCE, which possibly due to the increased free charge-carrier densities arising from the nitrogen doping in graphene. Moreover, the electrochemical behavior of EP with an anodic peak a1 and a pair of redox peaks (c2 and a2) at NG/CS/GCE is different from that on other pure graphene-based modified electrodes at pH 7.0, in which only an anodic peak a1^{12,15,31,43} or an anodic peak a1 and a cathodic peak c2⁴⁴ appears.

The electrochemical redox mechanism of EP has been reported in some works.^{9,41,45} It is generally considered to be a two electron-transferred reaction. In order to explain the redox mechanism of EP, the effect of the initial potentials and scan range in CVs was studied (Fig. S3). When we scanned in the range of $0.0 \rightarrow 0.5 \rightarrow -0.5 \rightarrow 0.0 \text{ V}$, all of the three peaks (a1, c2, a2) appeared (as shown in Fig. S3(A)). While we scanned in the range of $-0.1 \rightarrow -0.5 \rightarrow 0.5 \rightarrow -0.1 \text{ V}$, the couple of peaks (a2, c2) did not emerge until anodic peak (a1) came out (as shown in Fig. S3(B)). Next, when we scanned in the range of $-0.5 \rightarrow 0.0 \rightarrow -0.5 \text{ V}$, a pair of reversible peaks (a2, c2) still existed (as shown in Fig. S3(C)). Based on the previous work,⁴¹ the anodic peak (a1) corresponded to the electrochemical oxidation of epinephrine to open-chained quinone, and the open-chained quinone would partly transfer to adrenochrome. The cathodic peak (c2) owned to the reduction adrenochrome to leucoadrenochrome, while anodic peak (a2) corresponded to the oxidation of leucoadrenochrome to adrenochrome.

Moreover, as shown in Fig. 4, accompanied by the emerge of the cathodic peak (c2) and anodic peak (a2), the peak current of a1 decreased and that of cathodic peak (c2) increased in the second cycle scan compared to the first cycle. This result is consistent with the electrode reaction mechanism. The electrochemical redox process of EP can be occurred as follows:

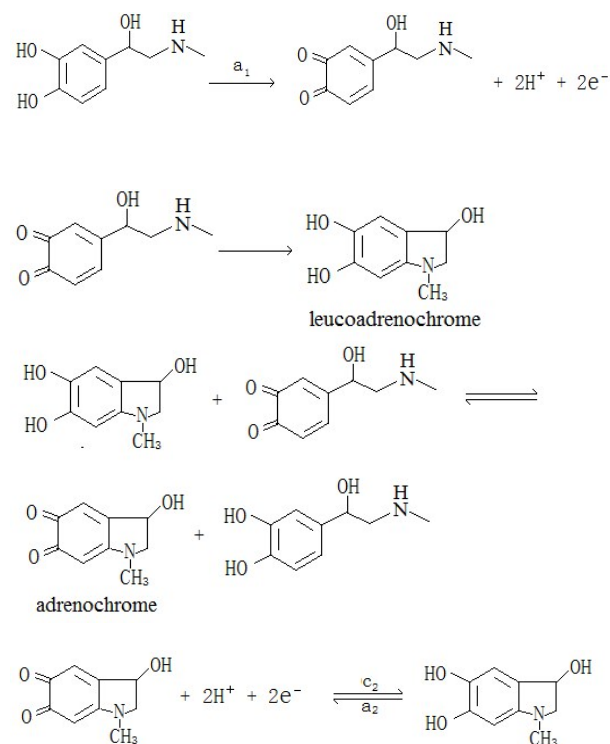


Fig. 5 shows the CVs of MEP at bare GCE and NG/CS/GCE in 0.1 M pH 7.0 PBS. An anodic peak (a1) and three cathodic peaks (c2, c3, c4) were found in the first cycle, while additional three anodic peaks (a2, a3, a4) appeared in the continuous second cycle at both bare GCE and NG/CS/GCE. The anodic potential of a1 at bare GCE was 550 mV, while it was 480 mV at NG/CS/GCE. That is, the overpotential of peak a1 reduced 70 mV at the modified electrode compared with that of the

Table 1 Comparing results for EP with different pure graphene-modified electrodes

Working Electrode	Solution pH	E_{pa}/V	LOD(M)	Linear range(M)	Reference
Nano-graphene-modified GCE	7.0	0.26	—	—	12
CVD graphene-modified GCE	7.0	0.47	—	—	15
Graphene nanosheets-modified GCE	7.4	0.28	—	—	31
Graphene-modified GCE	4.0	0.38	8.9×10^{-8}	3.85×10^{-7} to 1.09×10^{-4}	42
Porous graphene nanosheet-modified GCE	7.4	0.15	—	—	43
Graphene-modified Screen-Printed Electrode	7.0	0.40	6.56×10^{-7}	1.0×10^{-6} to 2.75×10^{-5}	44

NG/CS/GCE	7.0	0.18	6.7×10^{-7}	1.0×10^{-6} to 1.0×10^{-3}	This work
-----------	-----	------	----------------------	--	-----------

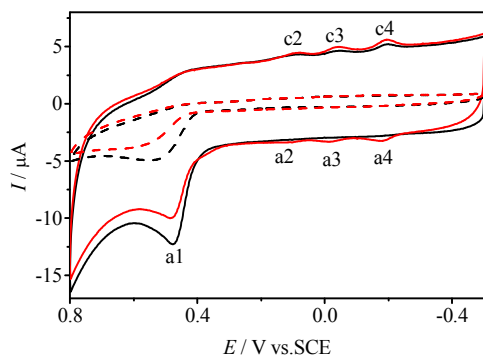
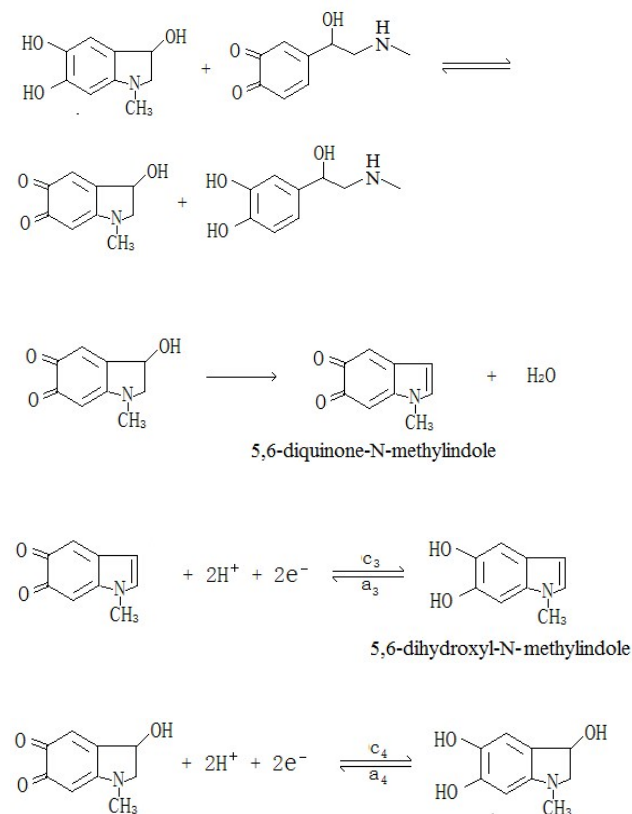
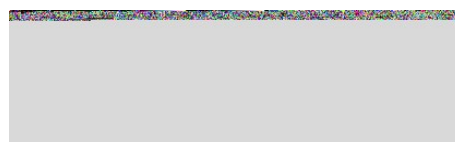
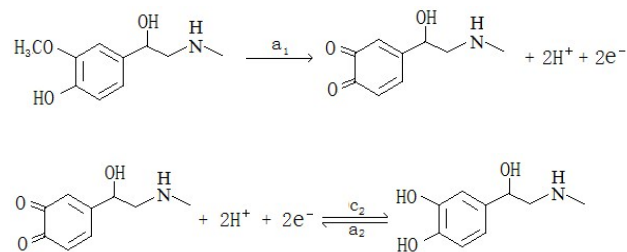


Fig. 5 CVs of 0.1 mM MEP at bare GCE (dash line) and NG/CS/GCE (solid line) (the black and red lines correspond to the first and continuous second cycle scan, respectively) in 0.1 M pH 7.0 PBS. Scan rate: 50 mV s^{-1} .

bare GCE. The redox peak currents of MEP enhanced dramatically at NG/CS/GCE. It demonstrates that NG/CS/GCE supplies a good electrochemical sensing platform for MEP due to the prominent property of NG.

Comparing with EP, the electrochemical behavior of MEP is seldom studied. Hence, we investigated the electrochemical redox mechanism of MEP as well. For clearly understanding the mechanism, we studied the effects of different initial potentials and scan potential ranges (Fig. 6). In the potential range of $0.25 \rightarrow 0.8 \rightarrow -0.5 \rightarrow 0.25 \text{ V}$, all of the redox peaks appeared in the first cycle (Fig. 6(A)). While we scanned in the range of $0.25 \rightarrow -0.5 \rightarrow 0.8 \rightarrow 0.25 \text{ V}$, only one oxidation peak (a1) came out in the first cycle. The three cathodic peaks (c2, c3 and c4) and three anodic peaks (a2, a3 and a4) did not appear until the occurrence of peak a1 (Fig. 6(B)). This demonstrates that the appearance of reduction peaks is indeed related to the oxidation of MEP. When we scanned in the ranges of $-0.5 \rightarrow -0.1 \rightarrow -0.5 \text{ V}$, $-0.5 \rightarrow 0.05 \rightarrow -0.5 \text{ V}$, and $-0.5 \rightarrow 0.2 \rightarrow -0.5 \text{ V}$, one pair (c4 and a4), two pairs (c4 and a4, c3 and a3) and three pairs (c4 and a4, c3 and a3, c2 and a2) of redox peaks emerged, respectively (Fig. 6(C)). It illustrates that, peaks a2 and c2, a3 and c3, a4 and c4 are reversible redox pairs, respectively. Considering the electrochemical behavior of EP in pH 4.0 PBS reported in the previous work,⁴¹ which also obtained three pairs of reversible peaks, we attributed a1 to the electrochemical oxidation of MEP to epinephrinequinone. Epinephrinequinone would be reduced to epinephrine (c2). Additionally, epinephrinequinone would partly transfer to 5,6-diquinone-N-methylindole and adrenochrome, which would be reduced to 5,6-dihydroxyl-N-methylindole and leuco-adrenochrome, corresponding to peaks c3 and c4, respectively. Meanwhile, anodic peaks (a2, a3 and a4) correspond to the oxidations of epinephrine to epinephrinequinone, 5,6-dihydroxyl-N-methylindole to 5,6-diquinone-N-methylindole and leucoadrenochrome to adrenochrome, respectively. Furthermore, Fig. 5 shows that the peak current of a1 in the second cycle scan decreased and that

of cathodic peaks (c2, c3 and c4) increased compared to those in the first cycle. This result further agrees to the proposed electrode reaction mechanism. The electrochemical behavior was proposed as follows:



3.2.2. Effect of scan rate

As can be seen in Fig. 7, the peak currents of EP and MEP increased sharply with scan rates ascending. According to the inset of Fig. 7(A), the peak current of a1 of EP was proportional to the square root of the scan rate ($r = 0.996$), which indicates

that the oxidation process is diffusion-controlled. The scan rate shows good linear relationships with the oxidation peak

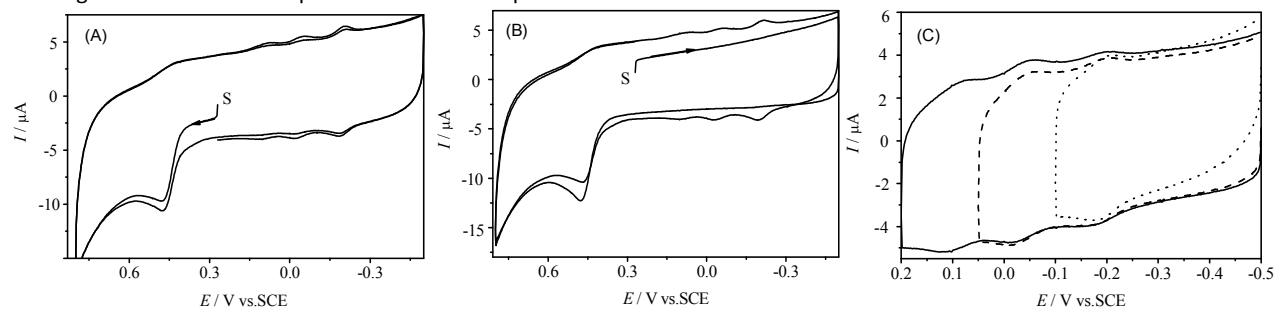


Fig. 6 CVs of 0.3 mM MEP with different initial potentials (A and B) and scan potential ranges (C) at NG/CS/GCE in 0.1 M pH 7.0 PBS at 50 mV s^{-1} , and S is the starting point of the potential scan.

current of a2 ($r = 0.998$) and reduction peak current of c2 ($r = 0.997$) of EP, demonstrating that the corresponding redox processes are adsorption-controlled. We supposed that, the larger conjugated regions, generated by the participation of the lone pair electrons in nitrogen atom of the five membered rings and benzene rings, lead to a stronger π - π interaction between adrenochrome (leucoadrenochrome) and NG. As to epinephrine, the absence of the N atom in conjugated regions yields a weak interaction. Thus the redox reactions of adrenochrome to leucoadrenochrome and leucoadrenochrome to adrenochrome were adsorption-

controlled electrochemical processes and the oxidation of epinephrine was a diffusion-controlled electrochemical process. Additionally, the analysis of $\log_{10} i_{pa2}$ versus $\log_{10} v$ reveals the gradient of 0.88, which is very close to "1", as is expected for a thin-layer effects within the electro-active species trapped in the 3D porous graphene network⁴⁰. From the inset of Fig. 7(B), there is a good linear relationship between anodic peak current of a1 of MEP and the square root of the scan rate ($r = 0.997$), which demonstrates that the oxidation of MEP at the modified electrode is a diffusion-controlled electrochemical process. For other peak currents of MEP were difficult to read, we only studied the effect of scan rate on peak a1 of MEP.

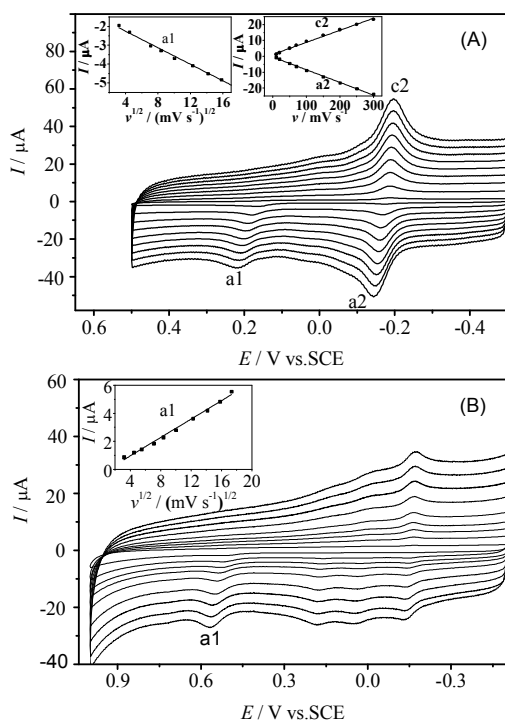


Fig. 7 CVs of 0.1 mM EP at different scan rates: 10, 50, 100, 150, 200, 250, 300, 350, 400 mV s^{-1} (from inner to outer) (A), and 0.1 mM MEP at different scan rates: 10, 30, 50, 70, 100, 150, 200, 250, 300 mV s^{-1} (from inner to outer) (B) in 0.1 M pH 7.0 PBS at NG/CS/GCE. Inset: plots of peak currents of EP (A) and MEP (B) vs. scan rate.

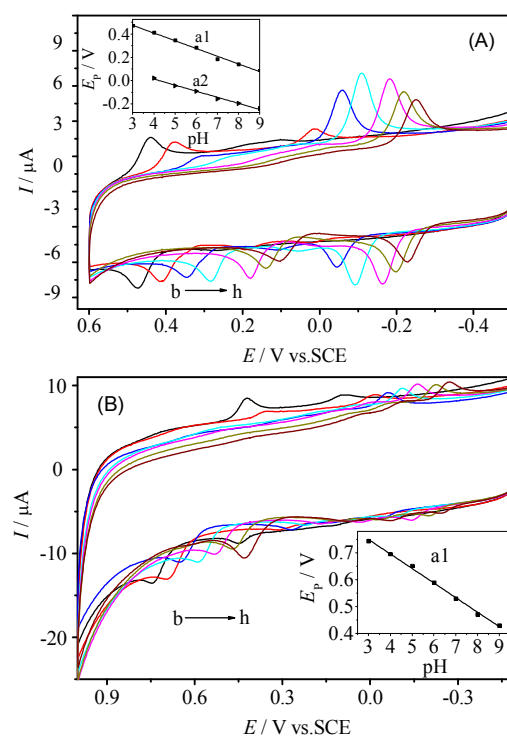


Fig. 8 CVs of 0.1 mM EP at 50 mV s^{-1} (A) and 0.1 mM MEP at 100 mV s^{-1} (B) in 0.1 M PBS with different pH values: 3.0, 4.0, 5.0, 6.0, 7.0, 8.0, 9.0 (from b to h) at NG/CS/GCE. Inset: plots of anodic peak potentials of EP (A) and MEP (B) vs. pH.

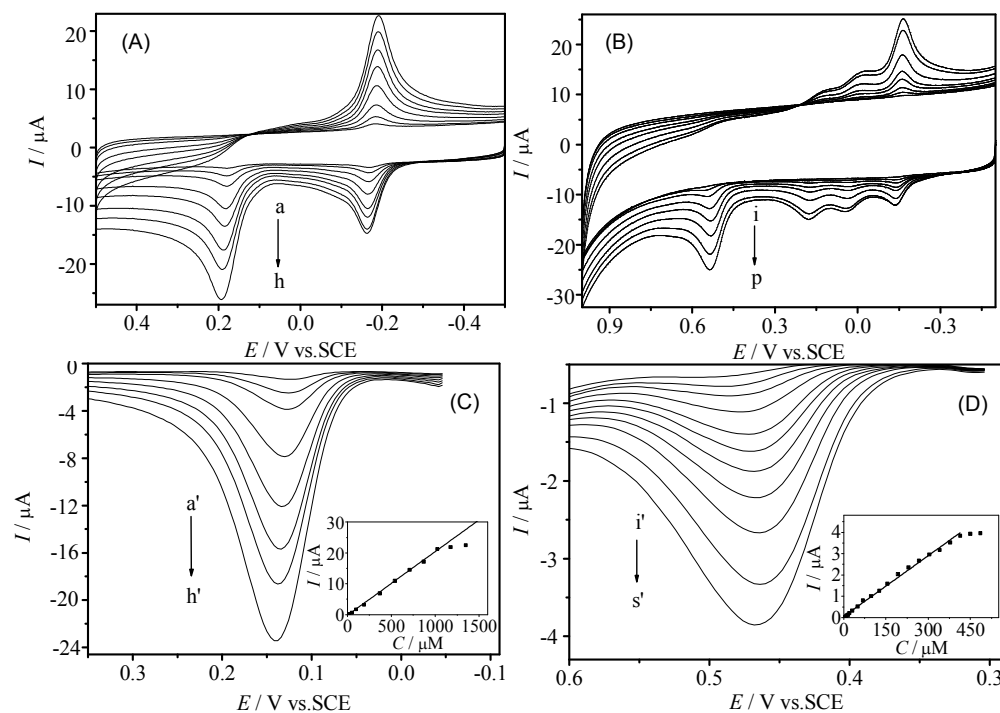


Fig. 9 CVs of NG/CS/GCE with different concentrations of EP: 3.0, 10.0, 30.0, 100, 200, 300, 400, 600 μM (from a to h) at scan rate: 50 mV s^{-1} (A), and MEP: 5.0, 10.0, 30.0, 50.0, 100, 200, 300, 400 μM (from i to p) at scan rate: 100 mV s^{-1} (B) in pH 7.0 PBS. DPVs of NG/CS/GCE with different concentrations of EP: 10.0, 30.0, 50.0, 200, 400, 600, 800, 1000 μM (from a' to h') (C) and MEP: 20.0, 30.0, 50.0, 70.0, 100, 130, 160, 200, 240, 320, 400 μM (from i' to s') (D) in 0.1 M pH 7.0 PBS. DPV conditions: increment potential 4 mV; pulse amplitude 50 mV; pulse width 0.2 s; pulse period 0.5 s. Insets: the calibration curves for EP (C) and MEP (D).

3.2.3. Effect of solution pH

Fig. 8 exhibits the cyclic voltammograms of EP and MEP in different pH values. Both of the anodic peak potentials of EP and MEP shifted negatively with the pH ranging from 3.0 to 9.0, which is a consequence of deprotonation involved in the oxidation process. The inset plot of Fig. 8(A) reveals the linear relationships between pH and anodic peak potentials of EP with the regression equations of $E_{\text{pa}1} = -0.0665 \text{ pH} + 0.675$ ($r = 0.996$) and $E_{\text{pa}2} = -0.0522 \text{ pH} + 0.221$ ($r = 0.995$). The slopes are 66.5 mV and 52.2 mV, which are similar to the theoretical value of 59 mV, indicating that the number of protons and electrons involved in the oxidation process is equal. This is consistent with the redox mechanism of EP aforementioned. The anodic peak potential of MEP ($E_{\text{pa}1}$) also has a linear relation with the pH values, with an equation of $E_{\text{pa}1} = -0.0540 \text{ pH} + 0.912$ ($r = 0.998$), as shown in the inset of Fig. 8(B). The slope of 54.0 mV indicates that the number of protons and electrons involved in the redox process is identical, which is coincident with the redox mechanism we have proposed.

3.3. Electrochemical detection of epinephrine and metanephrine

Fig. 9(A) and (B) display CVs of different concentrations of EP and MEP at NG/CS/GCE, respectively. We can see that, the peak currents enhanced with the increase of the concentrations of EP and MEP, while the peak potentials almost unchanged. Differential pulse voltammogram (DPV)

was applied for the detection of EP and MEP. Fig. 9(C) and (D) show a series of DPVs of EP and MEP with different concentrations, respectively. A series of well-defined voltammograms were obtained and with the concentrations increasing, the peak currents enhanced. The inset of Fig. 9(C) shows that the peak current has linear relationship with the concentration of EP from 1.0 μM to 1.0 mM, with the sensitivity of $0.021 \mu\text{A}/\mu\text{M}$ ($r = 0.996$). The limit of detection (LOD) was ascertained to be $0.67 \mu\text{M}$ ($\text{LOD} = (k \times b)/S$, $k = 3$, b is the standard deviation of blank solution noise signal and S is the slope of the calibration line). The inset of Fig. 9(D) shows that the peak current increased linearly with the increment of MEP concentration in the range of 1.5 μM to 0.41 mM. The sensitivity was $0.0095 \mu\text{A}/\mu\text{M}$ ($r = 0.998$) and the LOD was 1.3 μM . This sensor results for EP were compared with those on other pure graphene-based modified electrodes. In the previous reports, only two pure graphene-based modified electrodes (shown in Table 1) were investigated as the sensor for EP.^{42,44} The LOD for EP in this work is higher than that at graphene-modified GCE,⁴² almost same as that at graphene-modified Screen-Printed Electrode.⁴⁴ It should be specially stated that the sensor of graphene-modified GCE was used to detect EP with the electrolyte of pH 4.0⁴², different from of pH 7.0 here. The width of linear range for EP detection in this work is three orders of magnitude, same as that at graphene-modified GCE,⁴² larger than that at graphene-modified Screen-

Printed Electrode.⁴⁴ Generally, NG/CS/GCE exhibits good sensor results for EP and MEP.

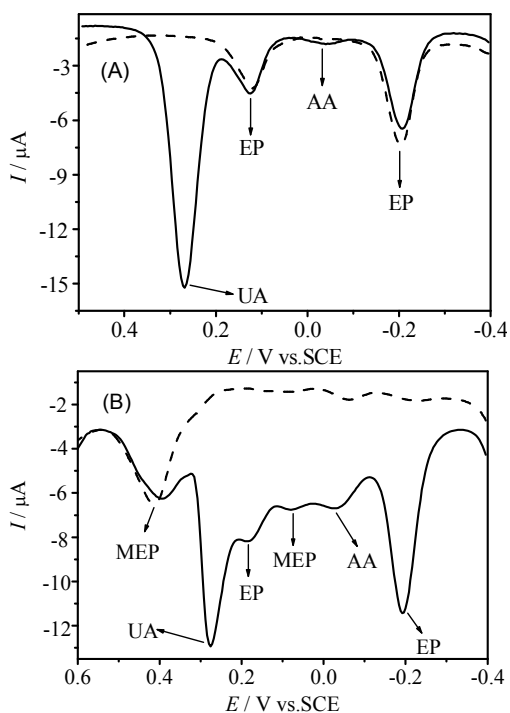


Fig. 10 DPVs of NG/CS/GCE in 0.1 M pH 7.0 PBS containing: (A) 0.1 mM EP (dashed line) and the mixture of 0.35 mM UA, 0.14 mM AA and 0.1 mM EP (solid line), and (B) 0.3 mM MEP (dashed line) and the mixture of 0.3 mM EP, 0.35 mM UA, 0.4 mM AA and 0.3 mM MEP (solid line). DPV condition parameters same as those of Fig. 9.

3.4. Interference study

It is well known that EP and MEP always coexist with UA and AA in the body fluids, and UA and AA usually interfere the detection of EP because of the overlaps of the oxidation waves. Here, the interferences of UA and AA for the detection of EP and MEP were investigated. As shown in Fig. 10(A) and (B), due to the low oxidation overpotential of EP at NG/CS/GCE, the anodic peaks of EP were separated from those of AA and UA and the anodic peak of MEP was distinguished with those of EP, AA and UA. In the previous reports at other pure graphene-based modified electrodes,⁴² it was investigated that the anodic peaks of EP and AA were distinguished. The distinguished anodic peaks imply that the interferences from UA and AA can be effectively eliminated for determining EP and those from EP, AA and UA for determining MEP. The tolerance limit was taken as the maximum concentrations of the foreign species which caused an approximately $\pm 10\%$ relative change in the detection. For the detection of 0.1 mM EP (by using the peak with peak potential at -0.2 V), the tolerated concentration of the foreign substances was 0.35 mM UA and 0.14 mM AA (Fig. 10(A)). For the detection of 0.3 mM MEP (by using the peak with peak potential at 0.4 V), the tolerated concentration of the foreign

species was 0.3 mM EP, 0.4 mM AA and 0.35 mM UA (Fig. 10(B)). The detection of EP and MEP in the presence of UA and AA were feasible at NG/CS/GCE in our experiment. However, the existence of MEP will affect the detection of EP.

3.5. Analysis application

To measure the practical application of NG/CS/GCE, recovery tests were carried out in human plasma samples and EP hydrochloride injections.

3.5.1. Analysis of human plasma samples

The human plasma samples were collected from volunteers and were diluted to 50 times with 0.1 M pH 7.0 PBS in advance. Different amounts of EP and MEP were spiked to plasma samples, respectively, and analyzed by DPV. The results obtained were summarized in Table 2. A satisfactory recovery (98.9% to 100.9%) was found. The recovery ratio turns out that the proposed modified electrode is effective in the detection of EP and MEP in human plasma samples.

3.5.2. Analysis of pharmaceutical samples

Three different batches of EP hydrochloride injections (stated amount of 1.0 mg mL⁻¹) were diluted to the proper consistency with 0.1 M pH 7.0 PBS separately and analyzed by DPV. Each batch was carried for three times and the recovery was determined respectively. The results were shown in Table 3. According the results of the diluted solutions content, the concentration of EP in the injections was calculated. The average determination results of EP in the injections were 0.991 mg/mL, 0.987 mg/mL, 1.09 mg/mL, respectively, which were quite coincident with the value that were given by injection specifications. The recovery varied from 100.3% to 104.6%, which indicates that NG/CS/GCE could be effectively used for the detection of EP in real samples.

3.6. Stability, reproducibility and repeatability

The stability, reproducibility and repeatability of NG/CS/GCE were investigated by CVs of 0.1 mM MEP. Parallel measurements were carried out using six modified electrodes. The relative standard deviation (RSD) was found to be 3.58%, proving that the modified electrode had excellent reproducibility. The repeatability of the modified electrode was evaluated by performing nine detection of 0.1 mM MEP, with a RSD of 2.85% which demonstrated good repeatability. The stability was studied by measuring 0.1 mM MEP after storing the modified electrode for ten days at 4°C in air. The peak current still remained 93.4% of the initial response, which illustrated good stability of the modified electrode.

Table 2 Detection results of EP and MEP in human plasma samples.

Number	Analyte	Added/ μ M	Found/ μ M	Recovery/%
1	EP	19.96	19.76	98.9
		69.51	68.82	99.0
		138.07	138.76	100.5
2	MEP	9.90	10.05	100.6
		39.84	39.73	99.7
		79.36	80.11	100.9

Analytical Methods Paper

Table 3 Detection results of EP in pharmaceutical samples

Sample	Content/ μM	RSD/% (n=3)	Added/ μM	Found/ μM	Recovery/ %
1	39.76	1.99	15.0	55.31	101.0
2	39.63	0.63	15.0	54.92	100.3
3	43.66	0.29	15.0	61.37	104.6

4. Conclusions

Nitrogen doped 3D porous graphene was fabricated and modified on GCE as biosensor for the detection of EP and MEP. NG/CS/GCE exhibited low anodic peak potentials and high current responses towards EP and MEP. The redox mechanisms of EP and MEP were also proposed, but further study was still needed for their complicated electrochemical redox processes, especially to MEP. The modified electrode can be applied to detect EP and MEP with excellent performance, which provides a good electrochemical sensing platform for analyses of EP and MEP.

Acknowledgement

Financial support from the National Natural Science Foundation of China (Grant Nos. 21175013 and 21174019) is gratefully acknowledged

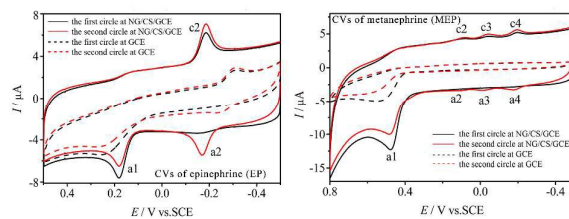
References

- 1 Y. Wang and Z. Z. Chen, *Colloids Surf., B*, 2009, **74**, 322–327.
- 2 J. D. Fernstrom and M. H. Fernstrom, *J. Nutr.*, 2007, **137**, 1539–1547.
- 3 R. Darr, C. Pamporaki, M. Peitzsch, K. Miehle, A. Prejbisz, M. Peczkowska, D. Weismann, F. Beuschlein, R. Sinnott, S. R. Bornstein, H. P. Neumann, A. Januszewicz, J. Landers and G. Eisenhofer, *Clin. Endocrinol.*, 2014, **80**, 478–486.
- 4 K. Pacak, G. Eisenhofer and H. Ahlman, *Nat. Clin. Pract. Endo.*, 2007, **3**, 92–102.
- 5 T. Deutschbein, N. Unger, A. Jaeger, M. Broecker-Preuss, K. Mann and S. Petersenn, *Clin. Endocrinol.*, 2010, **73**, 153–160.
- 6 B. Julie, G. Philippe and G. Blandine, *Eur. J. Endocrinol.*, 2013, **169**, 163–170.
- 7 S. Siva, G. Venkatesh, A. Prabhu and A. Muthu, *Phys. Chem. Liq.*, 2012, **50**, 434–452.
- 8 Y. S. Zhao, S. L. Zhao and J. M. Huang, *Talanta*, 2011, **85**, 2650–2654.
- 9 L. C. Figueiredo-Filho, T. A. Silva, F. C. Vicentini, and O. Fatibello-Filho, *Analyst*, 2014, **139**, 2842–2849.
- 10 Z. Ming, L. P. Guo, Y. Hou and X. J. Peng, *Electrochim. Acta*, 2008, **53**, 4176–4184.
- 11 A. A. Ensafi, F. Saeid, B. Rezaei and A. R. Allafchianb, *Anal. Methods*, 2014, **6**, 6885–6892.
- 12 X. Y. Ma and M. Y. Chao, *Anal. Methods*, 2012, **4**, 1687–1692.
- 13 A. K. Geim and K. S. Novoselov, *Nat. Mater.*, 2007, **6**, 183–191.
- 14 Rosy, S. K. Yadav, B. Agrawal, M. Oyama and R. N. Goyal, *Electrochim. Acta*, 2014, **125**, 622–629.

- 15 D. A. C. Brownson, M. Gómez-Mingot and C. E. Banks, *Phys. Chem. Chem. Phys.*, 2011, **13**, 20284–20288.
- 16 D. A. Brownson, C. W. Foster and C. E. Banks, *Analyst*, 2012, **137**, 1815–1823.
- 17 K. W. Chen, L. B. Chen, Y. Q. Chen, H. Bai and L. Li, *J. Mater. Chem.*, 2012, **22**, 20968–20976.
- 18 D. A. Brownson, L. J. Munro, D. K. Kampouris and C. E. Banks, *RSC Adv.*, 2011, **1**, 978–988.
- 19 D. A. Brownson, D. K. Kampouris and C. E. Banks, *Chem. Soc. Rev.*, 2012, **41**, 6944–697.
- 20 Y. Zhao, C. G. Hu, L. Song, L. X. Wang, G. Q. Shi, L. M. Dai and L. T. Qu, *Adv. Mater.*, 2014, **7**, 1913–1918.
- 21 Y. X. Xu, K. X. Sheng, C. Li and G. Q. Shi, *ACS Nano*, 2010, **4**, 4324–4330.
- 22 D. C. Brownson, L. C. Figueiredo-Filho, X. B. Ji, M. G. Mingot and C. E. Banks, *J. Mater. Chem. A*, 2013, **1**, 5962–5972.
- 23 D. Hulicova, M. Kodama and H. Hatori, *Chem. Mater.*, 2006, **18**, 2318–2326.
- 24 R. P. Rocha, A. G. Gonçalves, L. M. Pastrana-Martínez, B. C. Bordoní, O. S. G. Soares, J. J. M. Órfão, J. L. Faria, J. L. Figueiredo, A. M. T. Silva and M. F. R. Pereira, *Catal. Today*, 2015, **249**, 192–198.
- 25 R. Vinoth, S. G. Babu, D. Bahneman and B. Neppolian, *Sci. Adv. Mater.*, 2015, **7**, 1443–1449.
- 26 H. B. Wang, T. Maiyalagan, and X. Wang, *ACS Catal.*, 2012, **2**, 781–794.
- 27 X. R. Wang, X. L. Li, L. Zhang, Y. Yoon, P. K. Weber, H. L. Wang, J. Guo and H. J. Dai, *Science*, 2009, **324**, 767–771.
- 28 C. Dong, B. B. Jiang, K. L. Wu, Y. Hu, S. H. Xia and X. W. Wei, *Mater. Lett.*, 2015, **146**, 37–39.
- 29 J. Yan, R. W. Chen, Q. L. Liang and J. H. Li, *J. Nanosci. Nanotech.*, 2015, **15**, 4900–4908.
- 30 X. M. Feng, Y. Zhang, J. H. Zhou, Y. Li, S. F. Chen, L. Zhang, Y. W. Ma, L. H. Wang and X. H. Yan, *Nanoscale*, 2015, **7**, 2427–2432.
- 31 C. Z. Zhu, S. J. Guo, Y. X. Fang and S. J. Dong, *ACS Nano*, 2010, **4**, 2429–2437.
- 32 F. H. Cincotto, T. C. Canevari, A. M. Campos, R. Landers and S. A. S. Machado, *Analyst*, 2014, **139**, 4634–4640.
- 33 Y. Zhao, C. G. Hu, Y. Hu, H. H. Cheng, G. Q. Shi and L. T. Qu, *Angew. Chem. Int. Ed.*, 2012, **51**, 11371–11375.
- 34 Y. Q. Chen, L. B. Chen, H. Bai, L. Li, *J. Mater. Chem. A*, 2013, **1**, 1992–2001.
- 35 X. C. Dong, X. W. Wang, L. H. Wang, H. Song, H. Zhang, W. Huang and P. Chen, *ACS Appl. Mater. Interfaces*, 2014, **4**, 3129–3133.
- 36 D. A. Brownson and C. E. Banks, *The Handbook of Graphene Electrochemistry*, Springer, London, 2014.
- 37 D. A. Brownson, P. J. Kelly and C. E. Banks, *RSC Adv.*, 2015, **5**, 37281–37286.
- 38 L. C. Figueiredo-Filho, D. A. Brownson, O. Fatibello-Filho and C. E. Banks, *Electroanalysis*, 2014, **26**, 93–102.
- 39 R. G. Compton and C. E. Banks, *Understanding Voltammetry*, World Scientific Ltd., 1st edn, 2007.
- 40 P. M. Hallam, C. E. Banks, *Phys. Chem. Chem. Phys.*, 2011, **13**, 1210–1213.
- 41 H. S. Wang, D. Q. Huang and R. M. Liu, *J. Electroanal. Chem.*, 2004, **570**, 83–90.
- 42 X. Li, M. F. Chen and X. Y. Ma, *Anal. Sci.*, 2012, **28**, 147–151.
- 43 H. Wang, X. J. Bo and L. P. Guo, *Sens. Actuators, B*, 2014, **192**, 181–187.
- 44 I. M. Apetrei, C. V. Popa, C. Apetrei and D. Tutunaru, *Rom. Biotech. Lett.*, 2014, **19**, 9801–9809.
- 45 P. Kalimuthu and S. A. John, *Anal. Chim. Acta*, 2009, **647**, 97–103.

Table of contents

Low anodic potential was obtained in the detection of epinephrine and metanephrine with nitrogen doped three-dimensional porous graphene modified electrode.



1
2
3
4
5
6
7
8
9
10
11
12
13
14
15
16
17
18
19
20
21
22
23
24
25
26
27
28
29
30
31
32
33
34
35
36
37
38
39
40
41
42
43
44
45
46
47
48
49
50
51
52
53
54
55
56
57
58
59
60